

The Realization of a Novel Speed-Sensorless Induction Motor Drive

Ž. Janda, M. Janković, J. Bebić, S. Vukosavić, V. Vučković

Electrical Engineering Institute "Nikola Tesla"
Koste Glavinića 8a, 11000 Belgrade, Yugoslavia, phone 381-11-2351-412, fax 381-11-2351-823

Abstract - A simple low-cost controller for an induction motor has been implemented using a DC current sensor only. The fault current sensor is normally present in the DC link of an inverter for the protection purposes, and in this case it is used as the compensation signal source. Derived on such way, feedback signal has some amount of switching noise, which is successfully removed by a simple filter. After filtration, feedback current signal is converted into a digital value by means of an 8-bit A/D converter. The proposed controller uses a simple estimation procedure to maintain a constant rotor flux under steady state load conditions. Implemented algorithm is partially successful even during transient conditions. The speed torque characteristics obtained with proposed controller are tested on standard 7,5 kW motors, with different number of poles. Results are promising.

INTRODUCTION

The main goal of this paper is to describe the implementation of a low cost, speed-sensorless induction motor drive, based on the principles explained in an earlier paper [1]. According to classification given in [2], it belongs to general purpose drives.

The constant volt-seconds controlled induction motor drive system is widely used in various industrial fields, due to lack of expensive sensors, simple control algorithms and low cost implementations. Still, the speed sensitivity to load variations remains as a problem to be solved. Different solutions were proposed to keep the flux magnitude constant and the speed within narrow band. One such approach is presented in [4], where phase currents have been reconstructed from the observation of pulse currents existing in the DC bus of the PWM inverter. However, at low power factors the described technique produces underestimates of the motor current. The described signals have been derived by processing of the DC sensor signal through the network consisting of a lot of sample-and-hold circuits.

Somewhat similar approach have been introduced in [5], where the technique for reconstructing the motor line currents using information from a single current sensor in the DC bus is presented. All of the instantaneous motor currents can be

reconstructed with a bandwidth limited to half of inverter switching frequency. These current waveforms are used to produce a high-bandwidth signal proportional to the scalar magnitude of the motor current which is suitable for motor control purposes.

The results of further research are reported in [6], where the technique for the stator flux magnitude estimation in induction motor using DC link current is presented.

To the contrary of all described approaches, the one implemented in the presented realization is based on the DC link current measuring, but without extensive use of sample-and-hold circuits. The basics of the presented approach are reported in [1]. In such a way, the influence of the switching noise and switching aid circuits is reduced, since the reconstruction of the active current is dropped out. Instead, the flux is estimated in a more direct way. The penalty is slightly reduced overall performance.

Fig. 1 represents main parts of the drive. The drive consists of a half controlled thyristor bridge rectifier, variable frequency PWM inverter with IGBT transistors, squirrel cage induction motor (M), microcomputer system for control (MCS), braking device (B), Hall sensor for DC-current measurement (S), serial communication (SC), protection and other devices, as will be shown later.

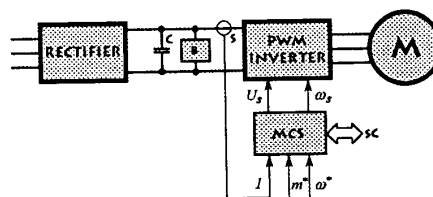


Fig. 1 - Simplified block diagram of the drive

The main task of the microcomputer system is to compensate for the motor slip changes caused by load variations and to maintain the pull out torque level, especially in the low speed region, when the influence of the stator resistance is increased. To accomplish this task the system uses a special algorithm based on a single measured value - DC current from the sensor S - giving corresponding corrections of inverter frequency and voltage [1]. The system also can be switched to maintain the constant torque instead of speed.

Besides that, the microcomputer system performs a series of other tasks – e.g., the generating of PWM signals for the inverter, communication with a computer or a higher level computer system by serial interface, communication with the user by keypad and display, automatic protection, etc.

2. POWER SECTION

Power section is built around the main heat sink carrying all power components and semiconductor modules. As inverter switches, insulated modules containing IGBT transistors are used. Mains supply side is built as three-phase half-controlled thyristor bridge, using insulated thyristor-diode modules. This bridge serves as a diode rectifier, but also as a thyristor rectifier that controls the inrush current during the start. In the DC link between mains side and motor side of converter an LC filter is inserted to suppress 300 Hz ripple component of link voltage, injected by input rectifier as well as the PWM ripple current. Power module drivers are built around specialized Siliconix IC Si9910, and short circuit protection is achieved by monitoring the collector-emitter voltage during conducting period of the power switch. In the fault case, control pulse width is automatically adjusted on minimal time (circa 2 μ s), but final inhibit of PWM driving signals is performed by control unit.

The main heat sink is force cooled by a fan supplied from the mains side. The heat sink temperature is controlled by a PTC resistor, with reacting temperature of 60°C.

Power module drivers are supplied with AC square wave voltage, obtained from common high frequency supply transformer with the screen. The primary winding of the transformer is supplied by a forward converter operated from 15 V supply of the main board. Transformer screen is connected to the power ground of the drive and ground points of EMI filters. Signal ground is connected to the power ground via high resistance in parallel with small capacitance. Also, the optocouplers used in power module drivers are internally screened.

The control electronics board is supplied via a stabilized DC/DC converter directly from DC link voltage.

3. CONTROL SECTION

The compensation of the stator resistance voltage drop is accomplished according to the following equations [1]:

$$\Delta u_s = K_u i_{dc}, \quad K_u \approx R_s \quad (1)$$

$$u_{s0} = K \omega_s, \quad K = L_s i_d \quad (2)$$

where R_s is stator resistance, ω_s angular stator frequency, i_{dc} DC link current, L_s stator inductance and i_d direct axis stator current in synchronous

reference frame. The compensated stator voltage signal is then:

$$u_s = u_{s0} + \Delta u_s = K \omega_s + K_u i_{dc} \quad (3)$$

The stator voltage control, based on the DC link current signal is expected to provide the constant flux operation in the wide speed area, since the presented equations are derived under approximations valid even at low speeds. The constant K in the voltage loop corresponds to the ratio V/f of the constant volt-seconds voltage-frequency characteristic.

Compensation of the speed drop, due to induction motor slip, under assumption of the constant rotor flux, is performed according to equation:

$$\Delta \omega_s = \omega_r = K_f (i_{dc} - I_f) \quad (4)$$

with the constants:

$$K_f = \frac{1}{(1 - \sigma) T_r i_d}, \quad I_f = \frac{i_d}{\sqrt{1 + \omega_s^2 T_s^2}} \quad (5)$$

where T_s and T_r are stator and rotor time constants and σ overall leakage coefficient.

It should be noted that K_f and I_f has no influence on the voltage loop, hence the selection of K and K_u is independent upon frequency loop parameters.

The simplified block diagram of both control loops is presented in Fig. 2.

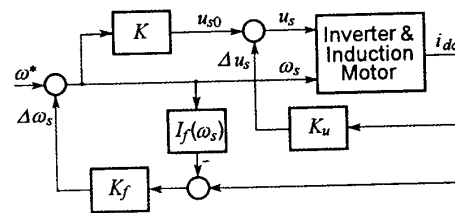


Fig. 2 - Simplified block diagram of the control

Control algorithm is implemented on 8-bit microcontroller 80535 and its digital environment, consisting of two 8254 timer modules, one 8255 PIA, one 27512 EPROM and one 28C64 EEPROM.

The software is written in assembler language of microcontroller 80535, except non time critical user interface routines, which are written in programming language C.

The flow diagram of the main routine, working in closed loop, is presented in Fig. 3, which is self-explanatory.

The interrupt routine for PWM has highest priority. It takes place every 1 ms, controlled by a separate timer. The PWM signals are generated by means of two programmable timer modules with six timers, three of which are for each transistor pair, one for reloading these timers and one for frequency dividing which is dependent on the chosen

modulation frequency (2 to 12 kHz, by steps of 2). The sixth one is not used. Normal SPWM with rectangular triangular carrier wave and sinusoidal reference, having injected third and multiples of third harmonic is used. In such a way the maximum modulation depth of line voltages is achieved [3].

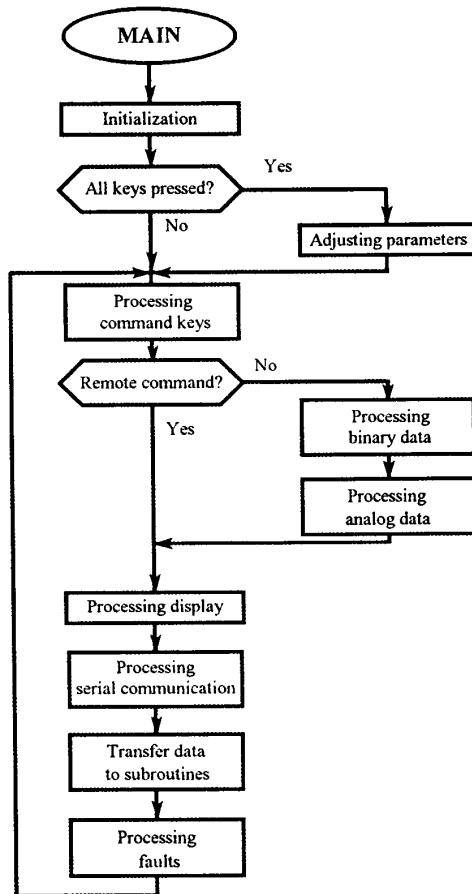


Fig. 3 – Simplified flow diagram of the main routine

The calculation of the PWM is optimized by speed and does not depend on the chosen modulation frequency. Calculated pulse width is rescaled immediately before loading of timer, using the tables stored in the EEPROM. In such a way the flow of calculation is straightforward and easy to implement.

While the second priority is given to the interrupt routine for serial communication, the routine for slip and torque control has the third priority. Initialized by an internal timer every 10 ms, this routine takes the data prepared by the main routine (commanded speed, acceleration and deceleration slope, commanded direction of rotation, commanded torque, etc.). After that, the checking of protecting signals is performed for the case when

the modulation inhibit is necessary. This protection includes the overvoltage, undervoltage, overcurrent, I^2t -level, motor and inverter overtemperature and break of the commanding current loop.

The next step is the A/D conversion of voltages from the potentiometers for reference speed and torque, as well as conversion of the DC link current from a Hall sensor and the DC voltage necessary for voltage protection and braking resistor control.

After that, the calculation of compensated speed and voltage is performed. In order to increase the speed of calculation of frequency and voltage corrections, tables stored in EEPROM are used. These tables are calculated and written into EEPROM during the process of parameter setting. It is important to note that the set of parameter values can always be adapted to the actual motor optimally.

Once calculated, the data for corrected speed and voltage are prepared for direct use by the PWM routine.

Finally, the control system has many additional features, that will be here only mentioned:

- acceleration and deceleration using speed ramp,
- DC overvoltage protection, performed on three ways:
 - by braking chopper
 - by control of deceleration ramp
 - by inhibiting the PWM modulation,
- supported RS 232 communication,
- monitoring of the heat sink temperature,
- monitoring of additional relay conditions,
- analog outputs for frequency and torque,
- possibility of master/slave connection (one drive is master, and it is adjusted to setpoint, while the second is slave, and operate only due commands received over the RS 232 link),
- programmable boost at low speeds.

These features mark the described drive for wide area of applications in industry.

4. PARAMETER SETTING

The field procedure of control parameter settings has several steps. It is necessary at first to calculate initial guesses for control parameters, using motor nameplate data and some simple field measurements. The rated frequency, voltage, speed and current are defined as program constants and can be directly entered in control program through the keypad (some default values are predefined, corresponding to maximal output capabilities of inverter and to European standards).

The stator copper resistance per phase should be measured by some appropriate method. The obtained value is then recalculated for the working temperature of the motor and normalized according to rated voltage and current. In such a way, the first

value of the constant K_u , defined in (1), is determined.

The initial value of the constant K_f in (4a) may be per-unit value of R_f . It can be seen from the expression (5a), after taking into account the expression (2b) and assuming per-unit values $L_r \approx L_s$, $K \approx 1$ and $s \approx 0$. This value can be obtained from the short circuit test on a standard way. It is useful, however, to perform this test by supplying the motor from the PWM inverter, in order to achieve both reduced voltage and low frequency. The initial per-unit value of the constant K in (2) is 1.

Of course, if the parameters of the motor (resistances and inductances) are available from the factory data, they can be directly used in formulas (1) to (5), after normalization, without any field measurements.

The second step consists of writing the constants into the control system using the keypad or a personal computer and its serial communication link, if available. The special preset routine of the microcomputer program calculates inverter switching patterns and writes the appropriate tables into EEPROM. After writing in a similar way the other operating data (e.g., desired speed, the acceleration ramp, etc.), the motor is started and run at no load under rated frequency. This will give the opportunity to eventually correct the value of the constant K . Then the slip is measured by means of some appropriate instrument (handheld tacho or stroboscope) under various loading conditions. Comparison with the slip obtained from nameplate data will give more accurate value of the constant K_f . The constant K_u is corrected in a similar way by supplying the motor with a frequency in the low region. Using the personal computer with a special auxiliary program, the described adjusting procedure can be automated.

Torque control is also implemented. Torque estimation is based on measured value of DC link current, and operating ω_s value. Developed algorithm for torque control is continuously comparing estimated torque value with the setpoint. If estimated value is higher, operating frequency is decreasing by the deceleration ramp slope, and if lower, operating frequency is increasing by the acceleration slope.

5. EXPERIMENTAL INVESTIGATION

Experimental investigations has been performed on the family of induction motors, fabricated by Yugoslav factory "SEVER", Subotica.

The main objective of testing was to confirm the improvement of the steady state mechanical characteristics in comparison with non compensated constant volt-seconds mechanical characteristics. All of the examined motors are of the 1.ZK132 type (frame size 132). In Fig. 4 the

family of slip-torque curves is shown under different supply voltage frequencies, without any compensation employed. The slip ω_{sl} is expressed relative to the rated synchronous angular frequency, and torque T_e relative to the rated torque. Motor type is 1.ZK132M4 (7.5 kW, 16 A, 3×380 V, 1440 rpm, number of poles 4). The non compensated curves lie within $\pm 1\%$ slip band only up to 40% of the rated torque, for the supply frequency range between 50 Hz and 10 Hz. For 5 Hz supply frequency case, it is visible that 40 % of rated torque is close to the pull out torque, so it is not possible to increase the motor load.

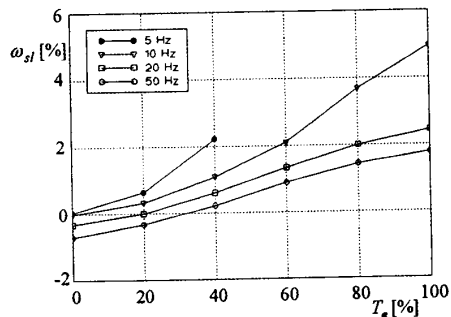


Fig. 4 - Slip vs. torque without compensation (4 poles)

With compensation employed, significant improvement of the mechanical characteristics is achieved. The corresponding family of absolute slip-torque curves is shown in Fig. 5. It is obvious that all curves are within the prescribed slip band.

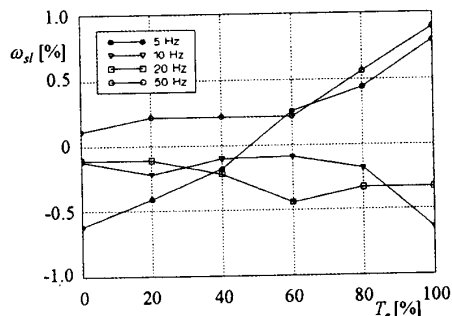


Fig. 5 - Slip vs. torque with compensation (4 poles)

Furthermore, the corresponding family of curves for the 2 pole motor 1.ZK132M2 (rated speed 2860 rpm) is shown in Fig. 6. Recorded curves correspond to the rated motor supply frequency and to the 10 % of rated motor supply frequency. During test the low damped speed oscillations during transients were observed, especially after sudden loss of load. Again the absolute slip band of $\pm 1\%$ has been achieved, as in the 4 pole case, but for different values of compensation parameters.

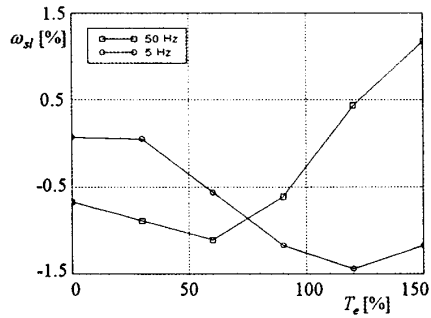


Fig. 6 - Slip vs. torque with compensation (2 poles)

Fig. 7 shows the test results with 6 pole motor of the same frame size (5.5 kW, 950 rpm). Recorded curves are again within $\pm 1\%$ slip band, but to the contrary of the 2 pole case, speed oscillations during transients were well damped.

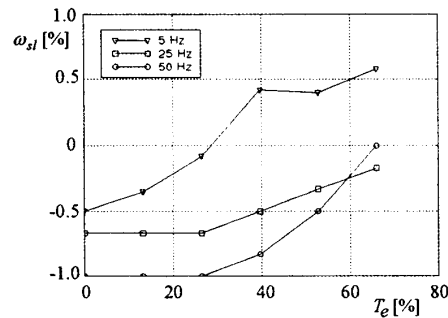


Fig. 7 - Slip vs. torque with compensation (6 poles)

As it can be seen on presented figures, the achieved speed error for load range from zero to nominal value, is within speed strip of $\pm 1\%$ of nominal speed.

Also, the transient characteristics for various SEVER motors are examined and elaborated. Test signal is torque step, up to 80% of nominal torque, and response signal is shaft speed.

The speed responses to the step load torque are shown in Figures 8, 9 and 10. Figures 8 and 9 show speed responses 25 Hz and 10 Hz supply frequency, respectively. In Fig. 10 the 5 Hz supply frequency case is shown, but load step is adjusted to be the 60 % of rated motor torque, to avoid pull out of the motor. This is done due to finite time necessary to elapse until flux level is rebuilt. Motor is not capable to withstand the sudden step load torque greater than temporary pull out torque. That fact was the main reason to reduce test load torque step in 5 Hz case, while under steady state load conditions, there were no similar problems. Elapsed time during speed recovery is dependent from supply frequency, as shown in appropriate figures.

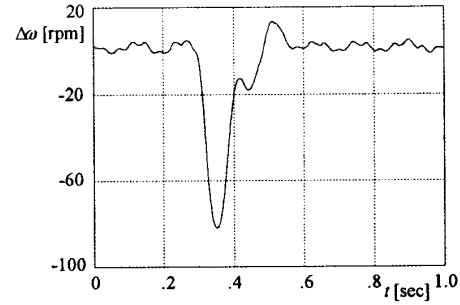


Fig. 8 - Speed response to the step of 80% rated torque (supply frequency is 25 Hz)

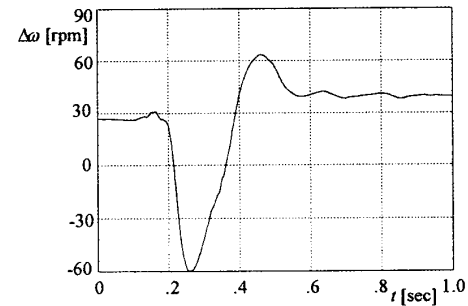


Fig. 9 - Speed response to the step of 80% rated torque (supply frequency is 10 Hz)

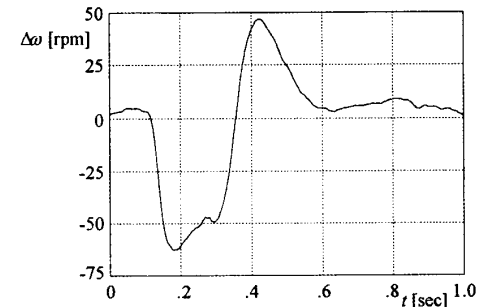


Fig. 10 - Speed response to the step of 60% of rated torque (supply frequency is 5 Hz)

6. CONCLUSIONS

A new low cost, completely digitally controlled general purpose AC drive with PWM inverter and induction motor is developed. The results of performed experimental investigations have confirmed the expected effectiveness of the new algorithm for slip and torque control, based on a single measurement of DC link current.

Further investigations are directed towards improvements of the dynamic behavior of the drive and towards extension of the torque capabilities at the speeds below 10 % of rated speed.

REFERENCES

- [1] V. Vučković, S. Vukosavić, "Control algorithm for the inverter fed induction motor drive with DC current feedback loop based on principles of the vector control", *Electric Machines and Power Systems*, 20:405-424, 1992
- [2] V. Stefanović, "Industrial AC Drives - Status of Technology", Survey Paper, *Proceedings of the 6th Conference on Power Electronics and Motion Control (PEMC '90)*, Vol.3, p.652, Budapest, 1990.
- [3] V. Stefanović, S. Vukosavić, "Space-Vector PWM Voltage Control with Optimized Switching Strategy", *IEEE IAS Annual meeting*, 1992.
- [4] J. T. Boys, "Novel current sensor for PWM AC drives", *IEE Proc.*, vol. 135, Pt. B, No. 1, Jan. 1988, pp. 27-32.
- [5] T. C. Green, B. W. Williams, "Derivation of motor line-current waveforms from the DC-link current of an inverter", *IEE Proc.*, vol. 136, Pt. B, No. 4, July 1989, pp. 196-204.
- [6] B. W. Williams, T. C. Green, "Steady-state control of an induction motor by estimation of stator flux magnitude", *IEE Proc.*, vol. 138, Pt. B, No. 2, March 1991, pp. 69-73.